these temperatures and subjecting the shields and linings to thermal relaxation to remove compressive strains in the layers from assembly, it is possible to significantly reduce contact heat transfer in the VSIC. In this case, there is an additional possibility for a reduction in the radiative component of heat transfer in the VSIC. This can be done by increasing the number of shields per unit thickness of the insulation to 20-25 shields/cm. Here, the compressive forces in the VSIC remain low.

NOTATION

Q_Σ, total heat flux; F, cross-sectional area; T, temperature; λ, thermal conductivity; ℓ, length; d, diameter; δ, thickness; $\dot{m}$ and $\dot{m}_0$, rate of evaporation of liquid nitrogen with and without the use of the cold of the vapors; R, service life of vessel before replenishment of cryogen; r, radius; x, coordinate along the throat. Indices: t, throat; pg, plug; in, insulation; gs, gas; ves, vessel.

LITERATURE CITED

1. G. G. Zhun', V. F. Getmanets, R. S. Mikhal'chenko, et al., Inzh.-Fiz. Zh., 54, No. 4, 600-607 (1988).
2. V. F. Getmanets, R. S. Mikhal'chenko, and P. N. Yurchenko, Inzh.-Fiz. Zh., 47, No. 4, 676 (1984).
3. B. J. Verkin, R. S. Mikhalchenko, V. F. Getmanets, and V. A. Mikheev, Proc. of 10th Int. Cryog. Eng. Conf., 529-538 (1984).
4. Low-Temperature Insulation, Inventor's Cert. No. 970025 SSSR: M. Kl.[3] G-17S3/02//F16 59/06.
5. Method of Thermally Insulating Cryogenic Devices: Inventor's Cert. No. 1262183 SSSR: 4F17S3/00.

TRANSPORT CALCULATIONS IN HYDROGEN STORAGE AS METAL HYDRIDES

G. A. Fateev, V. L. Tarasevich, V. Stanek, and P. Vychodil

UDC 536.433:629.113

A method is described for analyzing reactive transport in a metal hydride layer, which has been checked on a model for a hydrogen accumulator.

Hydrogen storage in hydrides formed by intermetallides has some advantages over traditional methods [1]; the hydrogen in these hydrides is stored under conditions close to normal, while the density may exceed that of liquid hydrogen. Compressed gases or cryogenic storage can produce analogous effects but require extreme conditions (high pressures or low temperatures). Additional advantages are that the hydrogen released from the hydrides is very pure and at high pressure.

These advantages are accompanied by limitations due to the delay in the transport in the layers, which means that the hydrogen accumulator is charged at a restricted rate (the device that provides the bound storage), and the same applies to the release rate. The desire to accelerate the exchange leads either to overheating the heat carrier or to complicated accumulator design, which increases the metal capacity because it is necessary to extend the interior surfaces. This means that one needs a careful analysis of the heat and mass transfer in the layers to optimize the design.

Hydrogen reacting with a hydride involves various transport mechanisms such as transport through the metallide layer, hydrogen-molecule dissociation at active surfaces (or

Lykov Institute for Heat and Mass Transfer, Academy of Sciences of the Belorussian SSR, Minsk. Institute for Chemical-Process Theory, Czechoslovak Academy of Sciences, Prague.

Translated from Inzhenerno-Fizicheskii Zhurnal, Vol. 57, No. 1, pp. 100-107, July, 1989. Original article submitted July 27, 1987.

0022-0841/89/5701-0811$12.50

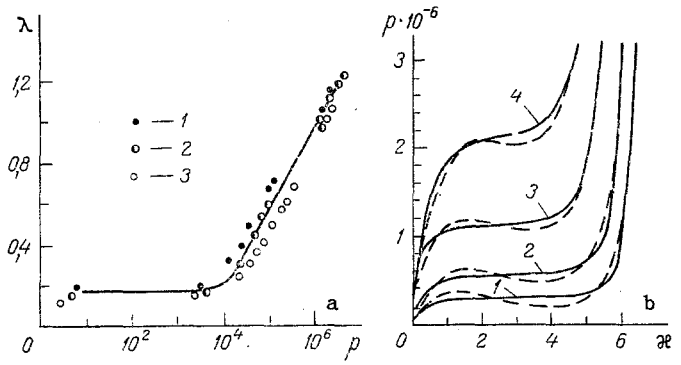

Fig. 1. Equilibrium and transport parameters for $LaNi_5H_x$: a) thermal conductivity as a function of hydrogen pressure at: 1) T = 363 K; 2) 333; 3) 303 K; b) equilibrium parameters in the $LaNi_5$-hydrogen system (solid lines from [4], dashed lines calculation from (1)): 1) T = 303 K; 2) 323; 3) 343; 4) 363 K; p in Pa, $\varkappa$ in atH/mol intermetallide.

recombination in hydrogen release), and hydrogen-atom diffusion in the lattice. Sometimes, the metal-hydrogen interaction alters the lattice.

These transport forms can be decisive in various systems; for example, when hydrogen reacts with certain metals or hot intermetallides, such as ones that release hydrogen at fairly high temperatures, dissociation and recombination tend to predominate along with activated diffusion. Correspondingly, metallide-hydrogen interaction tends to be of activted type, in which there can be critical phenomena in the reactive transport such as thermal explosion or hydrogenation-wave propagation [2].

When a low-temperature intermetallide such as $LaNi_5$ or FeTi interacts with hydrogen, the dissociation, recombination, and diffusion are comparatively rapid, while the rate-limiting step is the conductive transport, which is complicated by the energy-consuming transition of hydrogen into the hydride phases or conversely release from them. The energy transport in the intermetallide is determined by two specific factors: 1) the layer has a finely divided structure (the particle size becomes spontaneously a few microns after a sufficiently large number of hydrogenation–dehydrogenation cycles), and 2) the hydrogen in the structure may be in several states, e.g., in $LaNi_5$ there are two hydride phases virtually throughout the hydrogen content range. The first means that the effects from the gas pressure predominate over those from thermal conduction in the particle system, as molecular thermal conductivity in the filling gas tends to be decisive along with the conditions for interaction with the surfaces (Fig. 1a). The second factor, in accordance with Gibbs's rule, leads to the loss of a thermodynamic degree of freedom, which governs the specific power-law form for the isotherms and isobars (Fig. 1b). The degenerate equilibrium state is described [3] by

$$p = p_e F(\eta)/F(0{,}33), \quad p_e = p_\infty \exp(-\Delta h/RT), \tag{1}$$
$$F(\eta) = \eta/(1-\eta)\exp[\eta/(1-\eta) - \eta T_\Phi/T], \quad \eta = \varkappa/\varkappa_\infty.$$

Figure 1b compares measurements on equilibrium parameters for $LaNi_5$ with the (1) approximation [4]; the constants in (1) were taken as follows: limiting pressure (T = ∞) p_∞ = 4.17×10^{10} Pa, limiting mass content (p = ∞) $\varkappa_\infty = 7.66$ katom/kmol, phase transition energy $\Delta h = 3 \times 10^7$ J/kmol·K, and characteristic temperature governing the critical phase state T_p = 2557 K.

The coupled heat and mass transfer can be represented via the following model. The energy equation for the hydride layer is

$$\frac{\partial}{\partial \tau}\tilde{\rho}\tilde{h} = -\operatorname{div} q. \tag{2}$$

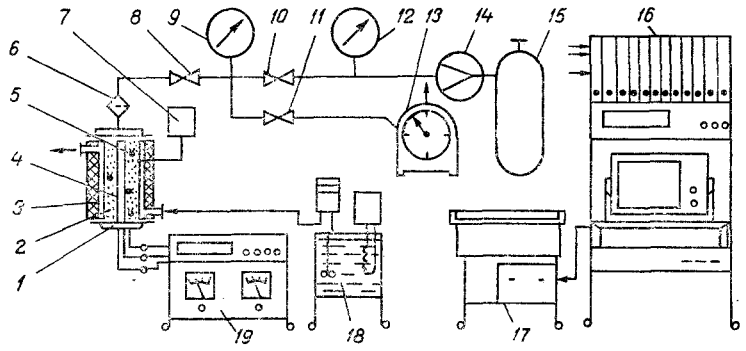

Fig. 2. Apparatus: 1) accumulator model; 2) working volume; 3) water jacket; 4) heater; 5) temperature sensors (couples); 6) filtering component; 7) TMD-25 pressure sensor; 8, 10, and 11) valves; 9 and 12) standard gauges; 13) gas meter type GSB-400; 14) RVD-5 M pressure reducer; 15) pressure vessel; 16) data-acquisition system; 17) printer; 18) NBE thermostat; 19) heater power supply.

The enthalpy of an elementary volume is made up of the enthalpies for hydrogen in the free and bound states and the enthalpy of the hydride:

$$\tilde{\rho}\tilde{h} = \tilde{\rho}_{H_2}\tilde{h}_{H_2} + \tilde{\rho}_H\tilde{h}_H + \tilde{\rho}_M\tilde{h}_M.$$

The bound-hydrogen density can be estimated from the atomic mass content $\varkappa$ in (1): $\tilde{\rho}_H \cong \tilde{\rho}_M \varkappa/2$.

The additional definitions

$$\begin{aligned} dh &= cdt - \Delta h d\tilde{\rho}_H, \\ c &= \tilde{\rho}_{H_2}\tilde{c}_{H_2} + \tilde{\rho}_H\tilde{c}_H + \tilde{\rho}_M\tilde{c}_M, \end{aligned} \tag{3}$$

lead us to represent the left-hand side in (2) as

$$\frac{\partial}{\partial\tau}\tilde{\rho}\tilde{h} = \left(\frac{\partial}{\partial\tau}\tilde{\rho}_{H_2} + \frac{\partial}{\partial\tau}\tilde{\rho}_H\right)\int \tilde{c}_{H_2}dt + \frac{\partial h}{\partial\tau}. \tag{4}$$

The right-hand side in (2) incorporates the conductive, convective, and filtration components of the heat flux $(q = -\lambda \operatorname{grad} t + h_{H_2}j_{H_2} + h_H j_H)$ and is written as

$$\operatorname{div} q = \operatorname{div}(-\lambda \operatorname{grad} t) + (\operatorname{div} j_{H_2} + \operatorname{div} j_H)\int \tilde{c}_{H_2}\,dt + \Delta h \operatorname{div} j_H + (j_{H_2}\tilde{c}_{H_2} + j_H\tilde{c}_H)\operatorname{grad} t. \tag{5}$$

We use (4) and (5) with the conservation equation

$$\frac{\partial}{\partial\tau}(\tilde{\rho}_{H_2} + \tilde{\rho}_H) = \operatorname{div}(j_{H_2} + j_H)$$

to write (2) as

$$\frac{\partial h}{\partial\tau} = \operatorname{div}(\lambda \operatorname{grad} t) - \Delta h \operatorname{div} j_H - (j_{H_2}\tilde{c}_{H_2} + j_H\tilde{c}_H)\operatorname{grad} t.$$

The diffusion fluxes $j_H = -D \operatorname{grad}\tilde{\rho}_H$, which we use to write the energy equation in the general form

$$\frac{\partial h}{\partial\tau} = \operatorname{div}\{\lambda[(1 - \mathrm{Le})\operatorname{grad} t - \mathrm{Le}/c \cdot \operatorname{grad} h]\} + (j_{H_2}\tilde{c}_{H_2} + j_H\tilde{c}_H)\operatorname{grad} t. \tag{6}$$

(6) corresponds to the equations used in describing reacting systems such as dissociated boundary layers [5], in which molecular and atomic gas components interact; (6) has been derived with the temperature and enthalpy as the transport potentials, in contrast to the traditional form of the energy equation in terms of enthalpy and concentration because under our conditions there is only a small contribution from macrodiffusion of the bound hydrogen in the finely divided system as regards the total energy transport, with the

transport characterized by a small value of Le. For simplicity, it is permissible to transform (6) on the assumption Le = 0. In some hydrogen accumulators, the hydrogen is supplied and tapped off in a way such that the gas filters through a layer having a low temperature gradient. We use the two assumptions (Le ≅ 0 and $j_{H_2}\,\tilde{c}_{H_2}\,\mathrm{grad}\,t \cong 0$) to represent (6) as

$$\partial h/\partial\tau = \mathrm{div}\,(\lambda\,\mathrm{grad}\,t). \tag{7}$$

(7) is written in terms of two potentials, and to represent the formulation in closed form, the two have to be related, with the relation representing the reaction kinetics during transition from the free state to the bound one or vice versa, as in [6]. In the present case, namely the interaction of hydrogen with a low-temperature intermetallide, there is no control effect from the reaction retardation, so one gets local equilibrium, and one can use the (2) equilibrium relation in the formulation. To establish how one can use the local-equilibrium condition, we represent (7) by means of (3) as

$$c\partial t/\partial\tau = \mathrm{div}\,(\lambda\,\mathrm{grad}\,t) + W. \tag{8}$$

The heat source is represented by the last term on the right in (8) and can be put as $W = \Delta h\,\partial\tilde{\rho}_{H}/\partial\tau$ or with the estimate $\tilde{\rho}_{H} \cong \tilde{\rho}_{M}\varkappa/2$ as

$$W \cong \frac{\Delta h\tilde{\rho}_{M}}{2}\,\frac{\partial\varkappa}{\partial t}\,\frac{\partial t}{\partial\tau}, \tag{9}$$

in which $\partial\varkappa/\partial t$ is defined on the corresponding equilibrium isobar and referred to the pressure established at the given moment. The power-law form of the equilibrium relations means that $\partial\varkappa/\partial t$ in (9) tends to be infinitely large near the plateau on the isobar, which corresponds to the phase transition localizing at a front at which there is a discontinuity in the first derivative of the temperature. Then (8) with (9) describes the energy balance at the front and the corresponding speed of that front:

$$c\,\frac{dn}{d\tau} = \nabla\cdot[(\lambda\,\mathbf{grad}\,t)\cdot\mathbf{n}], \tag{10}$$

in which n is the coordinate along the normal to the phase front. The right side in (10) defines the difference between the heat fluxes at the front, and it refers the treatment to a Stefan-type problem. There is a fairly effective method [7] of solving such problems for a phase transition in a metal hydride, but the analytic method is not capable of giving the full picture from the formulas applicable for practical estimates, particularly as regards all details of the equilibrium relations, and that not merely in the degenerate region, but also details of the boundary conditions under which the actual process occurs and possible complications in the interior-space geometry associated with extension of the heat-transfer surfaces. Therefore, more promise attaches to numerical methods of integrating the energy equation. One approach here consists in integrating that equation in two potentials in (7) directly by an explicit method [8, 9].

A major disadvantage in that approach lies in the limitations of the numerical explicit method, which are particularly notable in calculating reaction dynamics for hydrogenation-wave propagation [10] and also in multidimensional transport, which naturally arises in calculations on hydrogen accumulator design when there is an extensive internal heat-transfer surface.

We have therefore devised an inexplicit method for accumulator charging and discharging, which involves double fitting, where we use the energy equation containing a single potential (see (8)):

$$c_{ef}\,\frac{\partial t}{\partial\tau} = \mathrm{div}\,(\lambda\,\mathrm{grad}\,t),\quad c_{ef} = c + \frac{\Delta h\tilde{\rho}_{M}}{2}\,\frac{\partial\varkappa}{\partial t}, \tag{11}$$

and in which at each step it is assumed that the differential equation is linear, i.e., the coefficients are independent of temperature. The main conflict in that approach is that the effective specific heat in (11) is substantially dependent on temperature and becomes infinite at the transition front. A finite slope has been used in the program for computing the isobaric—isothermal parts of the equilibrium isobars, which represents a large but finite effective specific heat in (11).

Accumulator discharging is simulated from the solution to (12), which is integrated in dimensionless form:

$$c\frac{\partial t}{\partial \tau} - \frac{\lambda}{\rho}\operatorname{div}\operatorname{grad} t = \frac{\Delta h}{2M}\left(\frac{\partial \varkappa}{\partial \tau} - D\operatorname{div}\operatorname{grad}\varkappa\right). \tag{12}$$

The working space is cylindrical and the thermal conductivity is constant along the coordinate in an isobaric process, so the right side of (12) is taken as

$$\lambda\operatorname{div}\operatorname{grad} t = \lambda\left(\frac{\partial^2 t}{\partial r^2} + \frac{1}{r}\frac{\partial t}{\partial r}\right).$$

The following scales are used for the dimensionless quantities: temperature

$$t_* = t_W - t_0,\ t_W = t_0 + \frac{W}{2\pi\lambda l}\ln r_2/r_1, \tag{13}$$

in which W is heat of power and r_1 and r_2 are the coordinates for the working-space boundaries (heater and water-jacket radii); and for the bound-hydrogen mass transfer

$$\Delta\rho_* = \rho_{H0} - \int_V \rho_H\, dV\,|_{\tau=\infty},$$

in which ρ_{H_0} is the equilibrium mass content in the charged accumulator, while for the specific heat

$$c_* = c + \Delta h\Delta\rho_H/\Delta t;$$

and for the time

$$\tau_* = c_* r_1^2/\lambda;$$

and for the coordinate r_1, the heater radius.

(12) becomes in cylindrical coordinates and dimensionless variables

$$\frac{\bar{c} + \partial\bar{\rho}/\partial\bar{t}}{\bar{c}+1}\frac{\partial\bar{t}}{\partial\bar{\tau}} = \frac{\partial^2\bar{t}}{\partial\bar{r}^2} + \frac{1}{\bar{r}}\frac{\partial\bar{t}}{\partial\bar{r}}, \tag{14}$$

in which the dimensionless quantities are defined by

$$\bar{r} = r/r_1,\ \bar{c} = c/c_*,\ \bar{\tau} = \tau/\tau_*,\ \bar{\rho} = \rho/\Delta\rho_*,\ \bar{t} = t/t_*.$$

The $\bar{\tau}$ in (14) corresponds in meaning to the Fourier number:

$$\mathrm{Fo} = \lambda\tau\,[(c + \Delta h\Delta\rho_H/\Delta t)\, r_1^2]^{-1}.$$

The physical time scale implies considerable lag in the exchange in the layer under conditions of low thermal conductivity there, high phase-transition energy, and the small temperature differences arising with low-temperature intermetallides; this is a substantial limitation in bound hydrogen storage. For the same reasons, $\bar{c}$ in (14) is substantially less than one, and for qualitative analysis one can use

$$\left(\bar{c} + \frac{\partial\bar{\rho}}{\partial\bar{t}}\right)\frac{\partial\bar{t}}{\partial\bar{\tau}} = \frac{\partial^2\bar{t}}{\partial\bar{r}^2} + \frac{1}{\bar{r}}\frac{\partial\bar{t}}{\partial\bar{r}}. \tag{15}$$

The experimental methods described below and the dimensionless-quantity definitions give the boundary conditions as

$$\bar{t}(\bar{r},\ 0) = 0,\quad \bar{t}(\bar{r}_2,\ \mathrm{Fo}) = 0,\quad \partial\bar{t}/\partial\bar{r} = \bar{q}. \tag{16}$$

The assumptions made in the model are characteristic of phenomenological transport theory applicable to phase-transition cases; the geometrical characteristics defined by (16) may be made more complicated in accordance with design or technological requirements.

The method and its assumptions have been checked by a simulation based on a laboratory hydrogen accumulator.

Figure 2 shows the apparatus. The accumulator 1 has a cylindrical working volume 2, dimensions d = 0.038 m and ℓ = 0.175 m. The outer surface is thermostatically controlled by a coolant passed through the water jacket 3. Within the working volume, there is the coaxial heater 4, diameter 0.012 m. The intermetallide is placed in the annular gap 2 between the heater and the inner surface of the water jacket. We used an intermetallide of rare-earth type granulated on silicone rubber [11]. Within the working volume, there were temperature sensors 5 (Chromel–Copel thermocouples), whose readings passed to a microvolt-

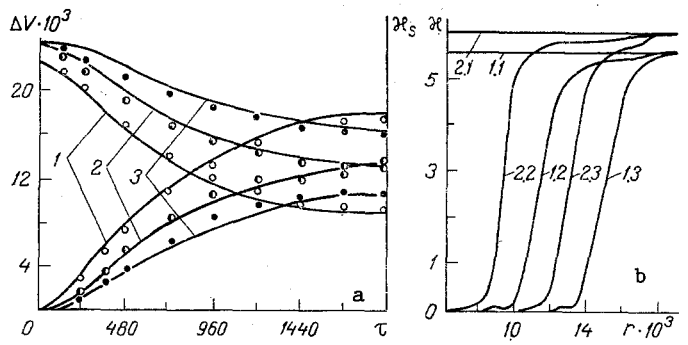

Fig. 3. Behavior of potential fields in metal hydride layer on discharging accumulator under isobaric conditions: a) mean integral mass content $\varkappa_S$ and hydrogen release volume ΔV for W = 60 W, pressure in MPa: 1) 0.3; 2) 0.5; 3) 0.7 (experiment); curves from numerical calculation for MPa of: 1) 0.3; 2) 0.5; 3) 0.7; b) concentration pattern calculations for p in MPa of: 1) 0.3; 2) 0.5; 1.1 and 2.1) τ = 0 sec; 1.2 and 2.2) 720; 1.3 and 2.3) 2400; ΔV and r in m^3.

meter in the data-acquisition system 16. The pressure was measured by the sensor 7 and gauge 9. The accumulator was connected to the hydrogen inlet and exhaust system 8-15.

The measurements were made as follows. Before the discharge, the device was thermostatically controlled at 20°C by passing the coolant from the thermostat 18 through the water jacket. Hydrogen was supplied from the cylinder 15 via the reduction valve 14 and valves 8 and 10 on the basis that the pressure in the accumulator was kept constant at the values set for the experiment. The charging was taken as completed when the pressure stabilized with the cylinder completely disconnected. Then the heater 4 was switched on and the discharging began, which involved isobaric hydrogen release through the valves 8 and 11 and the gas meter 13. The basic measured quantity was the hydrogen flow rate, but we also measured the temperature pattern in the working volume.

The model was checked by measurements at 3, 5, and 7×10^5 Pa; in that range, at 20°C we obtained virtually complete saturation in the intermetallide, and there were substantial differences in the discharge behavior for the integral nonequilibrium final state, in which the total capacity of the accumulator was not realized because the intermetallide layers adjoining the water jacket became almost completely saturated. The mass-content curves (Fig. 3) defined the widths of the phase-transition zones, which are localized in fairly narrow ranges near the front, which agrees with the above. The measurements agreed closely with the calculations, which confirms the method for computing the reactive transport.

One can thus calculate the hydrogen uptake and release in a metal hydride accumulator on the basis of the potential patterns in the intermetallide and the hydride phases by this method with acceptable accuracy.

NOTATION

c_m, specific heat, J/kg·K; D, diffusion coefficient, m^2/sec; j, specific gas flow rate, kmol/m^2·sec; Δh, heat of hydrogenation, J/kmol; h, enthalpy, J/kmol; p, pressure, Pa; q, specific heat flux, W/m^2; r, radius, m; R, universal gas constant, J/kmol·K; T and t, temperatures, K and °C; n, conversion factor; $\varkappa$, specific hydrogen content in hydrogen, at.H/mol intermetallide; $\tilde{\rho}$, molecular density, kmol/m^3; τ, time, sec; λ, thermal conductivity, W/m·K; Le = D/a, Lewis number. Subscripts: e, equilibrium, ef, effective, H, dissociated hydrogen in hydride, H_2, free hydrogen, m, metal or intermetallide, o, initial, W, wall, *, scale.

LITERATURE CITED

1. B. M. Smol'skii and N. M. Pashina, Heat and Mass Transfer: Physical Principles and Research Methods [in Russian], Sb. Nauch. Tr., ITMO Akad. Nauk Belorussian SSR, Minsk (1980), pp. 16-19.
2. D. A. Frank-Kamenetskii, Diffusion and Heat Transfer in Chemical Kinetics [in Russian], Moscow (1967).
3. V. V. Glushkov, V. L. Tarasevich, and G. A. Fateev, Aspects of Nuclear Science and Engineering: Atomic Hydrogen Power and Technology Series [in Russian], Issue 3 (19) (1984), pp. 54-56.
4. V. L. Tarasevich, Heat and Mass Transfer in Porous Bodies [in Russian], Sb. Nauch. Tr., ITMO AN Belorussian SSR, Minsk (1982), pp. 64-78.
5. W. H. Dorrens, Hypersonic Viscous-Gas Flows [Russian translation], Moscow (1966).
6. E. V. Agababyan, S. L. Kharatyan, M. D. Nersesyan, and A. G. Merzhanov, Fiz. Goreniya Vzryva, 15, No. 4, 3-9 (1979).
7. G. A. Fateev, A. I. Cheklina, and V. K. Shchitnikov, Vestsi AN Belorussian SSR, Ser. Fiz. Énerg. Navuk, No. 3, 26-30 (1981).
8. G. A. Fateev, Heat and Mass Transfer in Electrochemical Generators [in Russian], Sb. Nauch. Tr., ITMO AN Belorussian SSR, Minsk (1981), pp. 22-23.
9. V. L. Tarasevich, Thermophysical Processes in Power Plants [in Russian], Sb. Nauch. Tr., ITMO AN Belorussian SSR, Minsk (1982), pp. 158-163.
10. G. A. Fateev, Heat and Mass Transfer VII: Proceedings of the All-Union Conference on Heat and Mass Transfer, Minsk, May 1984 [in Russian], Vol. 3, Minsk (1984), pp. 163-169.
11. T. I. Derban, V. P. Mordovin, V. L. Tarasevich, and A. I. Cheklina, Physicochemical Processes in Nonequilibrium Systems [in Russian], Sb. Nauch. Tr., ITMO AN Belorussian SSR, Minsk (1986), pp. 113-126.

MATHEMATICAL MODELING OF PROCESSES OF PULSED MELTING AND VAPORIZATION OF A METAL WITH CLEARLY SEPARATED PHASE BOUNDARIES

P. V. Breslavskii and V. I. Mazhukin

UDC 519.63-536.422.1

The authors propose a method of numerical solution of problems of the Stefan type with two moving boundaries. As an example they solve the problem of pulsed melting and vaporization of an aluminum rod of finite length.

The pulsed action of concentrated energy fluxes on an absorbing solid medium has been considered in a number of monographs [1, 2]. On the whole, however, this problem is far from being resolved, due to a number of specific special features. The main feature is that an increase of the energy density supplied above a specific value leads to the development of complex phenomena in the solid, associated with nonequilibrium states and phase transformations. The description of these processes theoretically encounters a number of difficulties of a physical and mathematical nature.

The physical difficulties arise from the absence at present of a complete theory of nonequilibrium phase transformations and the inadequacy of experimental data.

The mathematical difficulties are associated with the fact that in a pulsed action, e.g., on a metal, one must consider, as a rule, the thermophysical characteristics of the substance and the two phase transformations. Analytical solutions of this kind of nonlinear problem are known, but are more frequently the exception, and the main methods of solving them are finite-difference methods [3]. Usually phase transitions of type I are described in the approximation of the classical Stefan problem [4], for which the main difficulties of

Im. M. V. Keldysh Institute of Applied Mathematics, Academy of Sciences of the USSR, Moscow. Translated from Inzhenerno-Fizicheskii Zhurnal, Vol. 57, No. 1, pp. 107-114, July, 1989. Original article submitted January 6, 1988.